

# We are IntechOpen, the world's leading publisher of Open Access books Built by scientists, for scientists

6,900

Open access books available

186,000

International authors and editors

200M

Downloads

Our authors are among the

154

Countries delivered to

TOP 1%

most cited scientists

12.2%

Contributors from top 500 universities



WEB OF SCIENCE™

Selection of our books indexed in the Book Citation Index  
in Web of Science™ Core Collection (BKCI)

Interested in publishing with us?  
Contact [book.department@intechopen.com](mailto:book.department@intechopen.com)

Numbers displayed above are based on latest data collected.  
For more information visit [www.intechopen.com](http://www.intechopen.com)



# Application of Computational Fluid Dynamics to Practical Design and Performance Analysis of Turbomachinery

Hyoung Woo OH  
Chungju National University  
Korea

## 1. Introduction

Over the past several decades, the meanline analysis method based on the conventional empirical loss correlations, assuming that the flow characteristics averaged over the cross-section of flow passage could represent the three-dimensional flow phenomena through the passage of turbomachinery, has been widely employed to determine the overall geometric design variables for each component of turbomachinery and to predict the on and off-design performance characteristics.

With the relentless increase in computing power, however, the computational fluid dynamics (CFD) techniques have remarkably progressed in the last decade, and CFD becomes commonly used not only as a design tool to improve the flow dynamic performance of specific components of turbomachinery but also as a virtual test rig to numerically experiment on a working prototype of the new/existing model.

This Chapter demonstrates how the meanline and CFD analyses can be applied to carrying out the hydraulic design optimization and performance analysis of a mixed-flow pump with the non-dimensional specific-speed ( $N_s$ ) of 2.44. Although the present article focuses on the incompressible flow machine, which falls into the regime of mixed-flow pumps with the non-dimensional specific-speed in the range of 1.9 to 2.5, the following procedure presented herein can be used efficiently as a practical design and analysis guide for general purpose turbomachinery.

## 2. Experimental apparatus for hydraulic performance

The Maritime and Ocean Engineering Research Institute (MOERI) constructed an apparatus (Fig. 1) to simulate the performance characteristics of the mixed-flow pump and conducted experiments on the hydraulic performance for the head rise, input power, pump efficiency versus flowrate, and the cavitation characteristics. The pump flowrate is calculated from the pressure difference across a downstream nozzle. Wall static pressures at the inlet and outlet planes are averaged in a manifold with four duct taps. The bulk total pressure, delivered head, is derived from the wall static pressure measurements and from the assumption of uniform velocity at the inflow and outflow stations. The input power is obtained from the torque transducer and impeller rotational speed readings. Uncertainties are  $\pm 1\%$  for head, flowrate, and shaft torque and  $\pm 1$  r/min for shaft speed.

Source: Computational Fluid Dynamics, Book edited by: Hyoung Woo OH,  
ISBN 978-953-7619-59-6, pp. 420, January 2010, INTECH, Croatia, downloaded from SCIYO.COM

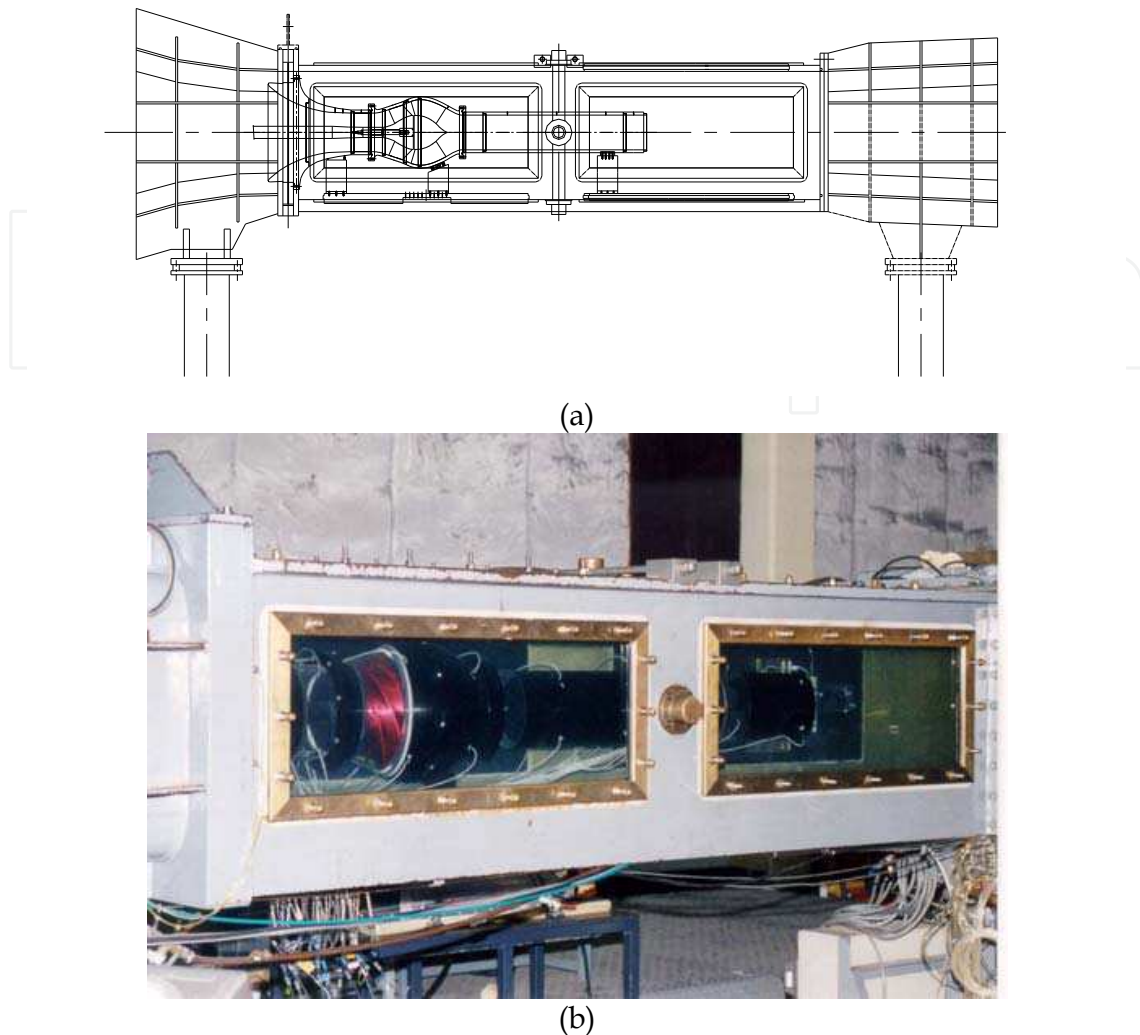


Fig. 1. Performance test rig: (a) schematic diagram and (b) view of test section section

### 3. Conceptual design considerations

In order to accomplish the specific geometric modeling of a three-dimensional configuration of turbomachinery, the overall configuration data have to be first specified, i.e. the inlet and outlet blade angles and other design variables for each component in the meridional plane have to be determined from the preliminary design process.

Most of the preliminary design and performance analyses of turbomachinery are still essentially empirical. General principles on the design theories of fluid machinery based on empirical loss correlations have been well described in a number of references (Aungier, 2000; Japikse, 1994; Neumann, 2005; Stepanoff, 1993). However, because the open literature provides only the ranges of design variables such as the ratios of inlet to outlet diameters, the inlet and outlet blade angles as a design guide, the specific values of the design variables in the recommended ranges have to be determined to achieve a design point performance target by design engineers' own past experience.

The present study adopted the meanline design code (Oh & Kim, 2001) in order to carry out the conceptual design optimization of a mixed-flow pump. This program states the loss of mixed-flow pump efficiency as an objective function and then deals with a nonlinear

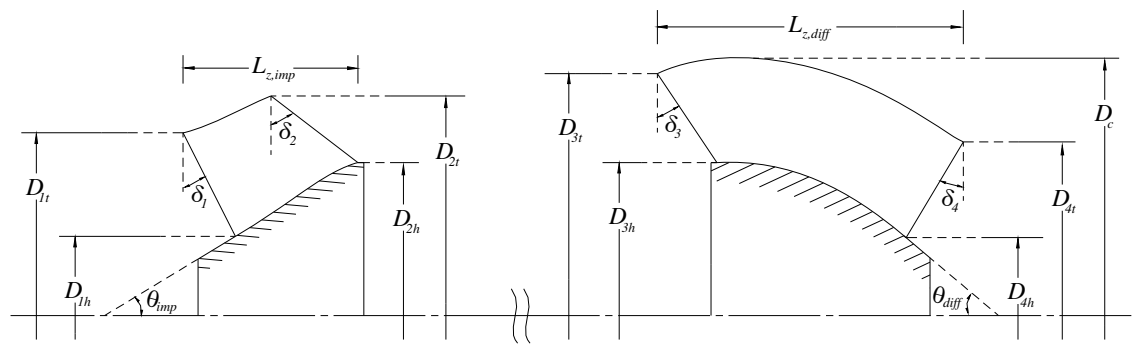


Fig. 2. Meridional cross-section of mixed-flow pump with geometric parameters

constrained optimization problem – most of the geometric and fluid dynamic design constraints herein are, unfortunately, based on the industrial field data and designer’s database. Figure 2 depicts the overall meridional configuration of a mixed-flow pump system with representative geometric parameters. Taking account of the design target in this study, the pump system should satisfy the performance of the head coefficient ( $\psi \equiv 6.5 \times gH / (\Omega^2 D_{in}^2)$  where  $g$  is the gravitational acceleration [m/s<sup>2</sup>],  $H$  is the pump total head [m],  $\Omega$  is the rotational speed [rad/s], and  $D_{in}$  is the inlet duct diameter [m]) 0.557 at the flow coefficient ( $\phi \equiv 5 \times Q / (\Omega D_{in}^3)$  where  $Q$  is the volume flow [m<sup>3</sup>/s]) 0.747 as a mixed-flow pump with the non-dimensional specific-speed of 2.44. The non-dimensional specific-diameter ( $D_s$ ) of the mixed-flow pump preliminarily optimized by using the meanline analysis is 1.79, which lies on the collected field data (Balje, 1981) of efficient turbomachines (Fig. 3). This confirms that the present conceptual design optimization for the meridional

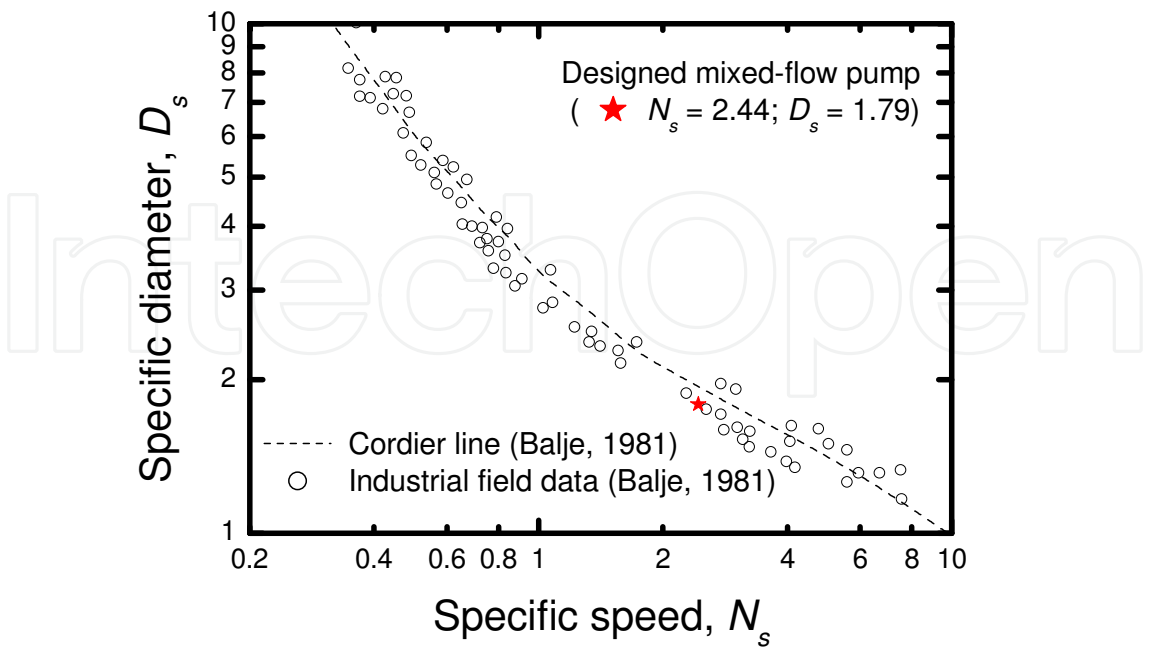


Fig. 3. Specific-speed and specific-diameter diagram

configuration has been accomplished within the reliable design regime. As a reference, the Cordier line (Balje, 1981), which is a fair curve through the field data in the statistical sense, is represented in Fig. 3.

## 4. Detailed design optimization and performance analysis using CFD

### 4.1 Overview of design process

The detailed design work on the impeller and diffuser blades proceeds in consideration of the overall meridional geometric data determined from conceptual design optimization. The present study decides the three-dimensional configuration by using a well-established commercial CFD package (ANSYS 12.0 Turbo System, 2009), whose predictive capabilities to analyze the performance characteristics of a variety of turbomachines have already been validated in the open literature and industrial applications, that enables the user to create a new blade geometry and to analyze the three-dimensional viscous flow phenomena within the blade passage in a graphical environment. Investigating the internal flow dynamics and the performance characteristics of a pump system, the iterative design process is continued until geometric feasibility is reached.

Some representative design factors to be first considered in accomplishing detailed design optimization can be briefly stated as follows: The blade angles along the streamline should be distributed in such a way that the blade-loadings, i.e. the static pressure difference between the blade upper and lower surfaces, are optimized along the blade surface and the incidence, defined as flow angle minus blade angle, has to be designed to improve the pump efficiency and the pump performance at the off-design points. In the case of diffuser, to suppress the energy dissipation due to the exit swirl, the blading has to be achieved to minimize the rotational velocity component at the exit of diffuser.

Newly designed impeller and diffuser for a mixed-flow pump in accordance with the above detailed design procedure are illustrated in Fig. 4.

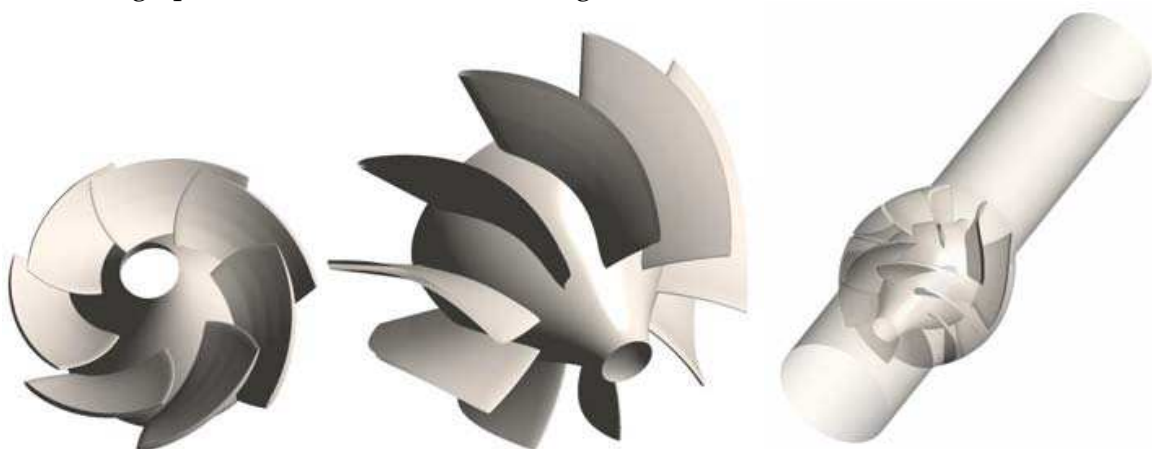


Fig. 4. Three-dimensional modeling: impeller (left), diffuser (middle), and a mixed-flow pump stage for computation (right)

### 4.2 Computational aspects

The right side of Fig. 4 shows the three-dimensional modeling for the performance analysis of a mixed-flow pump stage. The computational domain is divided into the inlet duct, the unshrouded-impeller with tip-clearance, the diffuser, and the outlet duct parts, with a total



number of 1 237 287 nodes and 1 176 622 hexahedral elements, of which the size next to the wall boundary has been determined to meet the required condition,  $y^+ \leq \sim 3$ , for highly accurate boundary-layer simulation. This grid system as shown in Fig. 5 is used for all subsequent computations. In order to remove the dependence of the solution on the grid density, the simulations were run on a number of meshes of different mesh refinement such as 1 031 877, 1 237 287, 1 248 185, and 1 344 297 nodes.

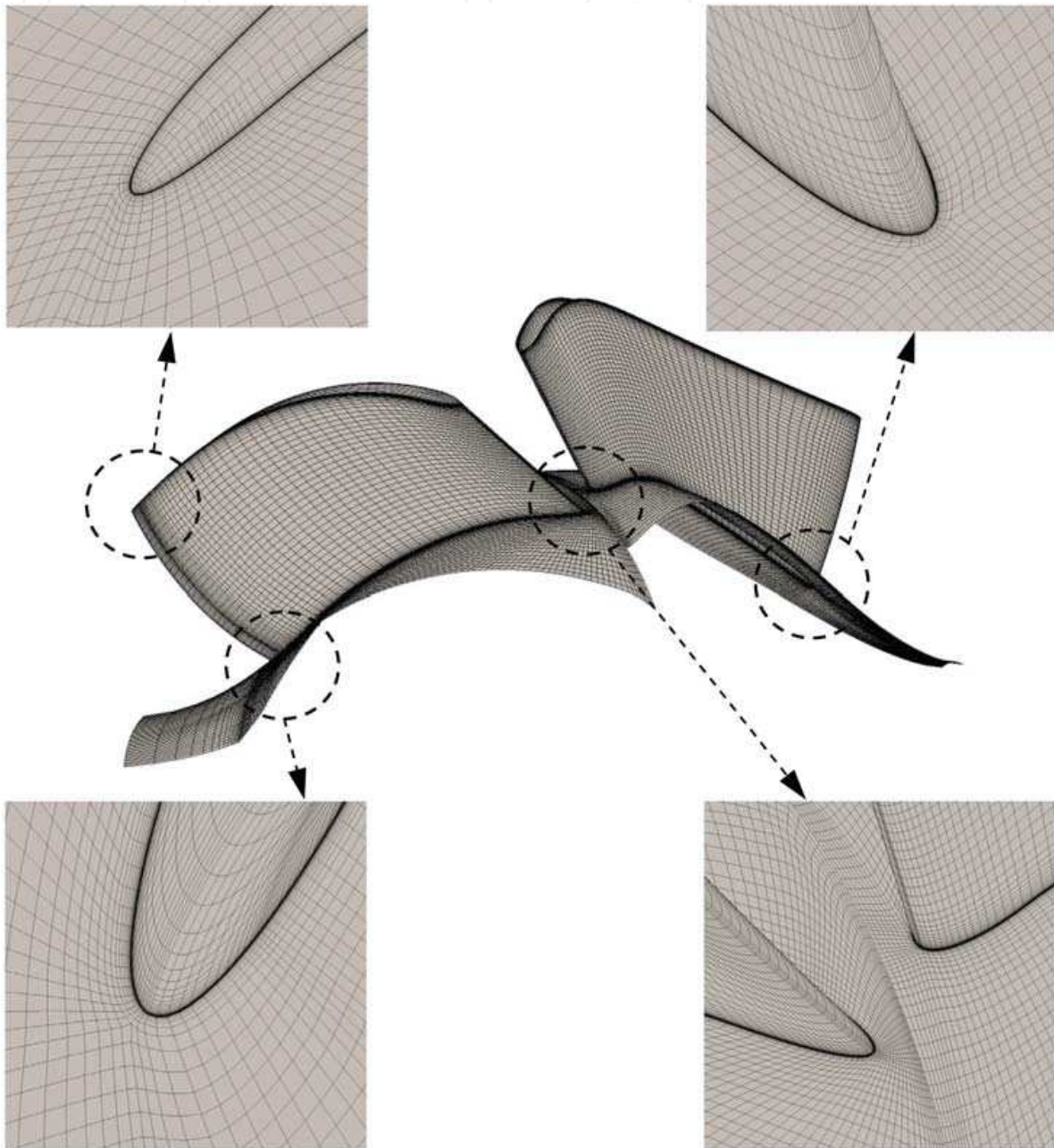


Fig. 5. View of computational mesh for impeller and diffuser

The numerical analysis of three-dimensional steady-state turbulent flow based on the Reynolds-averaged Navier-Stokes equations has been performed using the  $k-\omega$  based shear stress transport model to give accurate predictions of the onset and the amount of flow separation.

As for the boundary conditions, the total pressure was prescribed at the inflow boundary, whereas the mass flowrate was specified at the outlet section of the pump stage. The inlet duct, diffuser, and outlet duct were set as absolute stationary. The surfaces of the unshrouded-impeller blade and hub were the relative stationary except for the impeller shroud casing wall, which was modeled as stationary in the absolute frame of reference. All computations have been carried out using water at 25 °C as a working fluid.

A multiple frame of reference calculation with a general grid interface, which permits non-matching of node location, element type, surface extent, surface shape, and flow physics across the connection, solves a series of both rotating and stationary components, and the flow passing through the frame-change interface called a stage or mixing-plane interface is calculated by averaging the flux in the circumferential direction, although the variation in the meridional plane is preserved. Moreover, the rotationally periodic boundary conditions for each component with one blade passage are implemented in order to reduce the computational mesh size of the mixed-flow pump stage.

#### 4.3 Internal flow characteristics at design flow and off-design performance curves

A computational study has been carried out to determine the performance characteristics of a mixed-flow pump under the normal operating conditions. Figures 6 to 8 show the representative flow dynamic phenomena for the design flowrate in a mixed-flow pump developed by the present design and analysis method. Here, the notation 'ii' means the interface between the inlet duct and the impeller, and 'id' does the interface between the impeller and the diffuser. In addition, 'do' denotes the interface between the diffuser and the outlet duct. Figure 6(a) illustrates the computed streamwise static and total pressure (normalized by the atmospheric pressure) distributions through the flow passage in the pump stage. The overall performance curves gradually increase and then level out. Observing the static pressure distribution in the diffuser part, the static pressure rises as the flow diffuses because of the expansion of flow area, and the local flow acceleration caused by the curvature near the hub region of the diffuser exit leads to a slight fall in the static pressure distribution.

In order to decrease the total pressure loss, i.e. the energy dissipation due to the exit swirls of a pump stage, or to improve the pump efficiency, the rotational (or tangential) component of the absolute velocity through the diffuser and outlet duct passages has to be minimized. As can be seen in Fig. 6(b), the calculated absolute flow angle (measured from the meridional plane) remains satisfactorily constant at around  $-2.1^\circ$ , which represents that the diffuser blading has been obtained to eliminate the swirling flow in the outlet of the pump stage.

Figures 7(a) and 8(a) show that the blade-loadings for the static pressure (normalized by the atmospheric pressure) are ideally distributed along the streamlines of the impeller and the diffuser over the blade-span, although the flow reversal phenomena appear near the exit regions, which is substantially regarded as the flow separation. In Figs. 7(b) to (d), the relative flow streamlines on the impeller blade surfaces have been well optimized without any separation lines. However, the elliptic configuration for the impeller trailing edge and the centrifugal force induced by the impeller rotation give rise to the flow separation along the trailing edge, and the secondary flows due to vortex-curling over the impeller blade tip affect the flow separation on the pressure surface of impeller near around 75% blade-span.

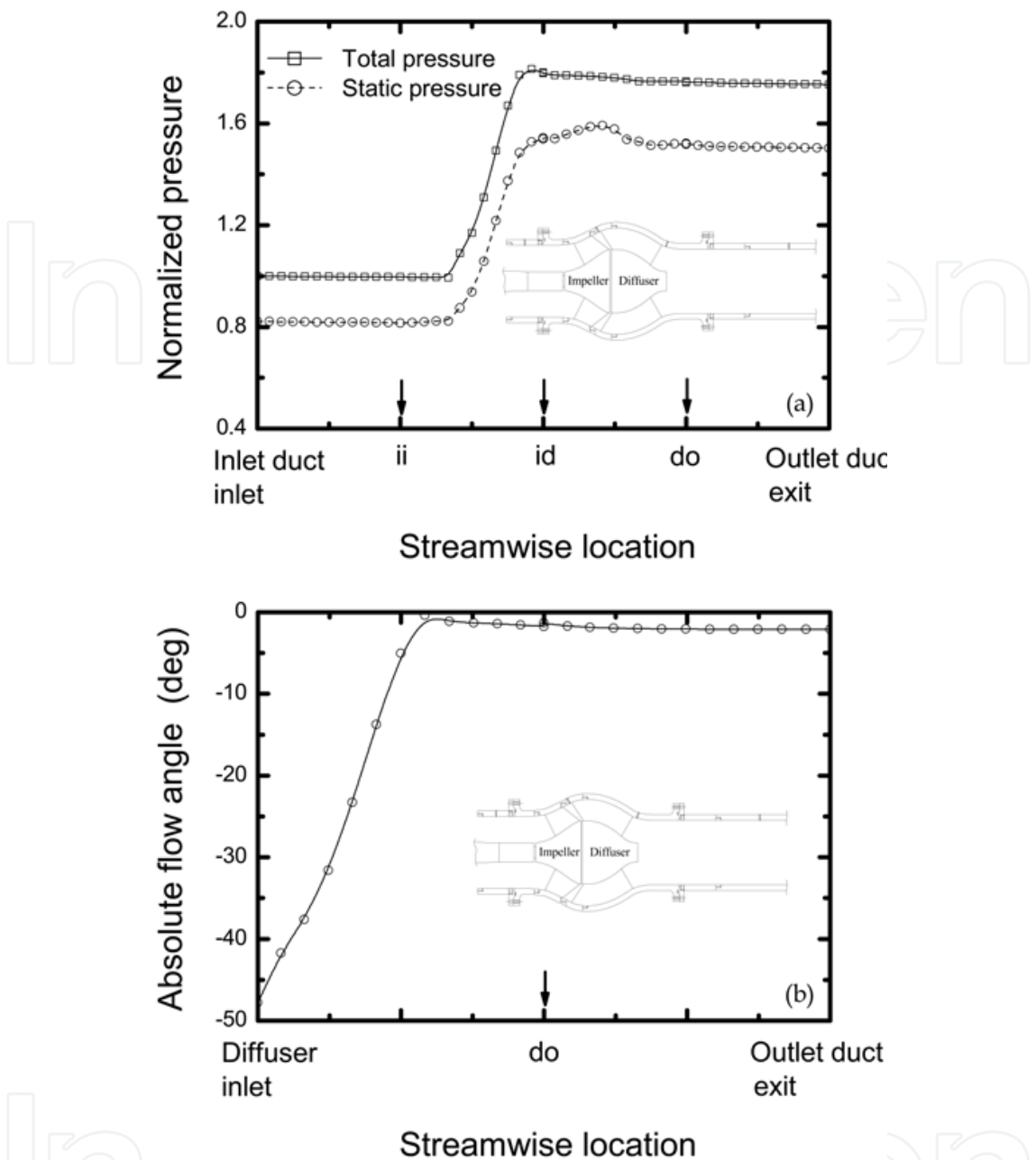


Fig. 6. Streamwise flow characteristics of a mixed-flow pump: (a) static and total pressure distributions, and (b) absolute flow angle distribution

As for the absolute streamlines on the diffuser blade, it is observed from Figs. 8(b) to (d) that except at the pressure side, the excessive flow separation appears near the exit hub region of the suction side, which is due to the adverse pressure gradient along the streamwise direction and the curvature around the exit hub region of the diffuser passage.

A comparison between the computed and measured performance characteristic curves of a mixed-flow pump is illustrated in Fig. 9. Here is the torque coefficient ( $\tau$ ) defined as  $30 \times \dot{W} / (\rho \Omega^3 D_{in}^5)$  where  $\dot{W}$  is the input power [W] and  $\rho$  is the fluid density [kg/m<sup>3</sup>], and the pump efficiency ( $\eta$ ) defined as  $\rho g H Q / \dot{W}$ . As shown in this figure, the experimental data agree very satisfactorily with the predicted performance curves in a range of operating flow conditions.



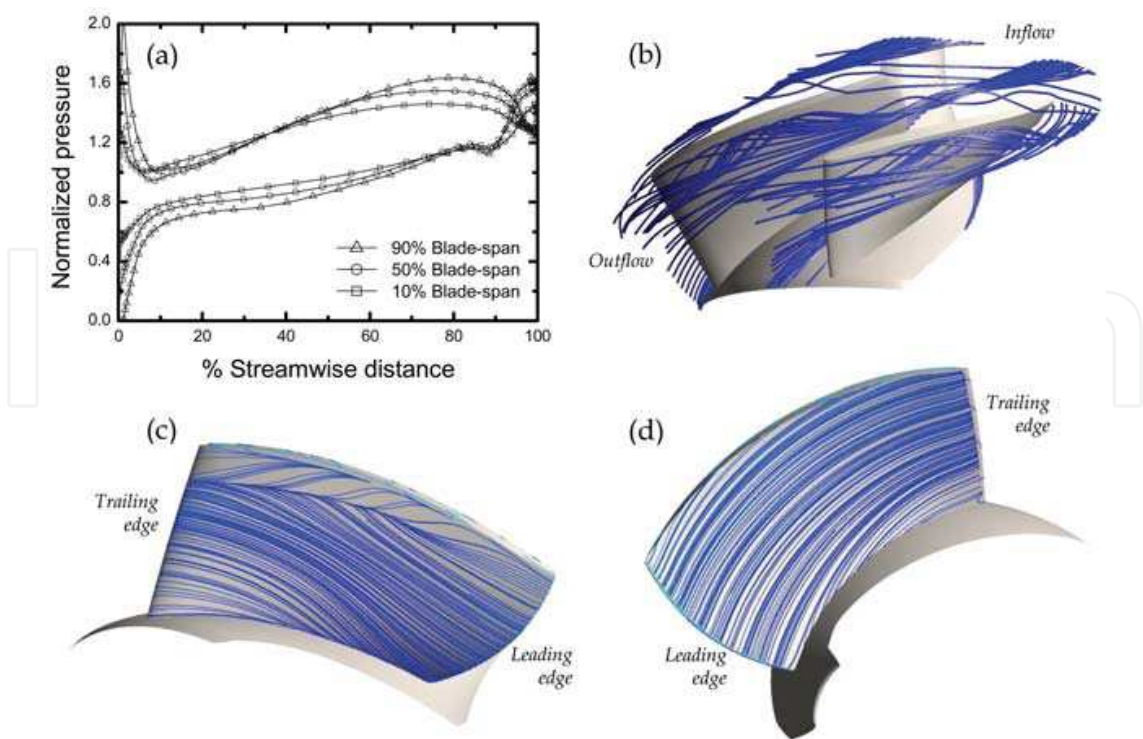


Fig. 7. Flow dynamic phenomena around the impeller blade: (a) blade-loading distributions (b) streamtubes for the overall flow, (c) streamline distribution on the pressure side, and (d) streamline distribution on the suction side

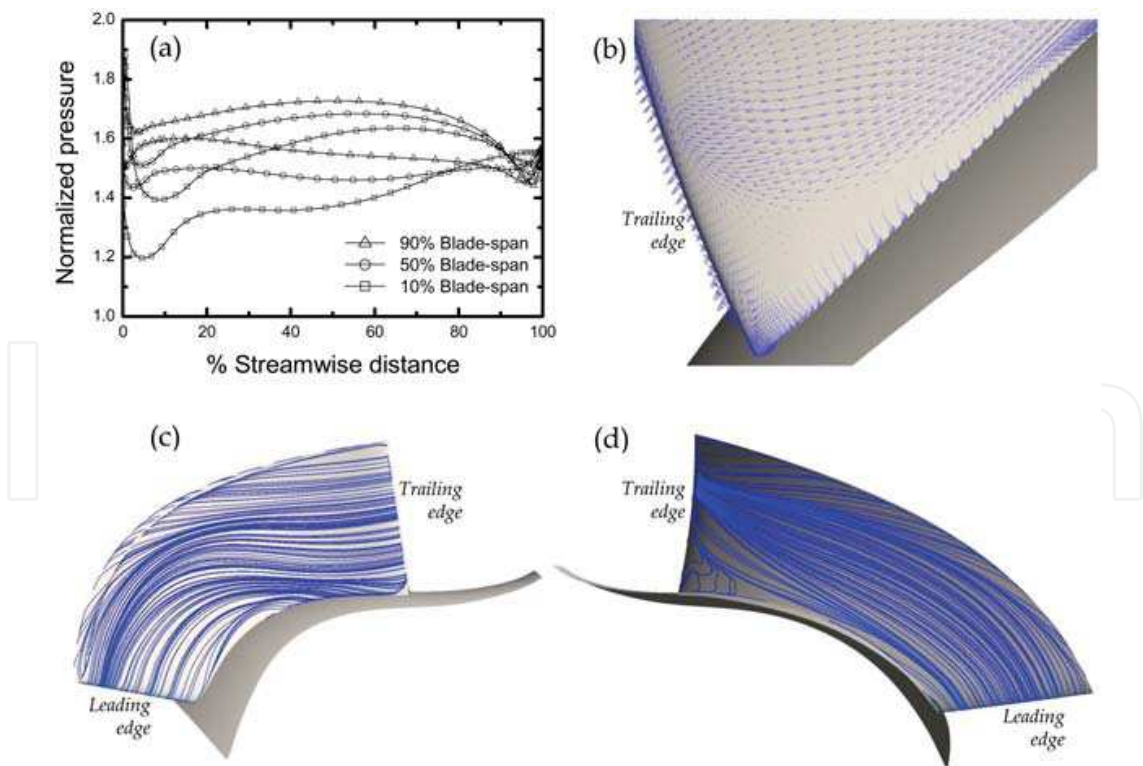


Fig. 8. Flow dynamic phenomena around the diffuser blade: (a) blade-loading distributions, (b) velocity vectors near the exit hub of the suction side, (c) streamline distribution on the pressure side, and (d) streamline distribution on the suction side

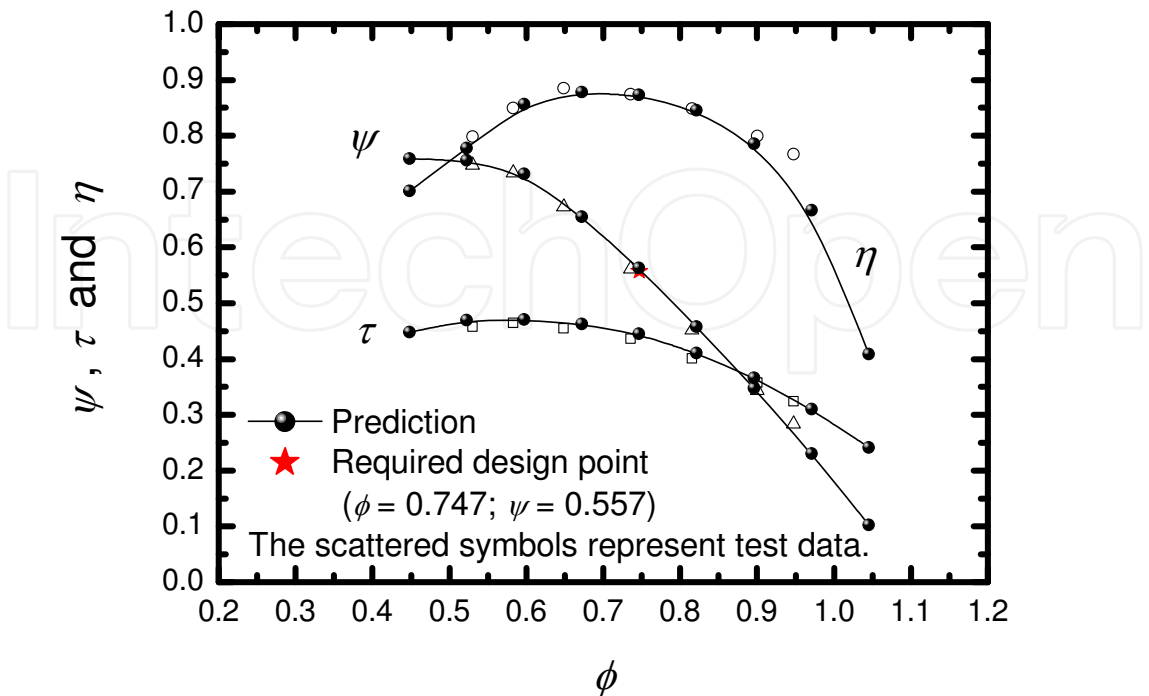


Fig. 9. The performance characteristic curves of a mixed-flow pump

4.4 Cavitation performance characteristics

Generally, cavitation occurs in the liquid system when the local absolute static pressure in a flowing liquid is reduced to or below the vapour pressure of the liquid, thereby forming vapour bubbles. The bubbles suddenly collapse as they are convected to a high-pressure region. The consequent high-pressure impact may lead to hardware damage, e.g. local pitting and erosion, and emit noise in the form of sharp crackling sounds. Cavitation may also degrade the performance characteristics of hydraulic machinery.

Figure 10 demonstrates the cavitation performance characteristic curves of a mixed-flow pump developed by the present optimal design method, considering the highest pump efficiency. In order to investigate the flow dynamics of cavitation for the near-design flowrate ( $\phi = 0.738$  in Fig. 10) under the design pump speed, the side-view of the cavitating flow along the impeller blade has been photographed through the window of the test facility and compared with the isosurface plots, generated by the CFD code, for the vapour fraction of the fluid. In this figure, the cavitation parameter ( $\sigma$ ) is defined as the ratio of the net positive suction head (NPSH) to the pump total head. At case (1), a small amount of cavitation, the inception of cavitation, occurs at the tip vortex generated by the tip of the impeller leading edge. With further reduction up to case (4) in the cavitation parameter, the tip-vortex cavitation has been more produced; the generated pump head still remains, however, constant without severe performance degradation. When the NPSH reaches a sufficiently low value over the knee of nearly constant head coefficient (for case (6)), the distortion of the flow pattern, by mixing more tip-vortex and face sheet cavitation with the

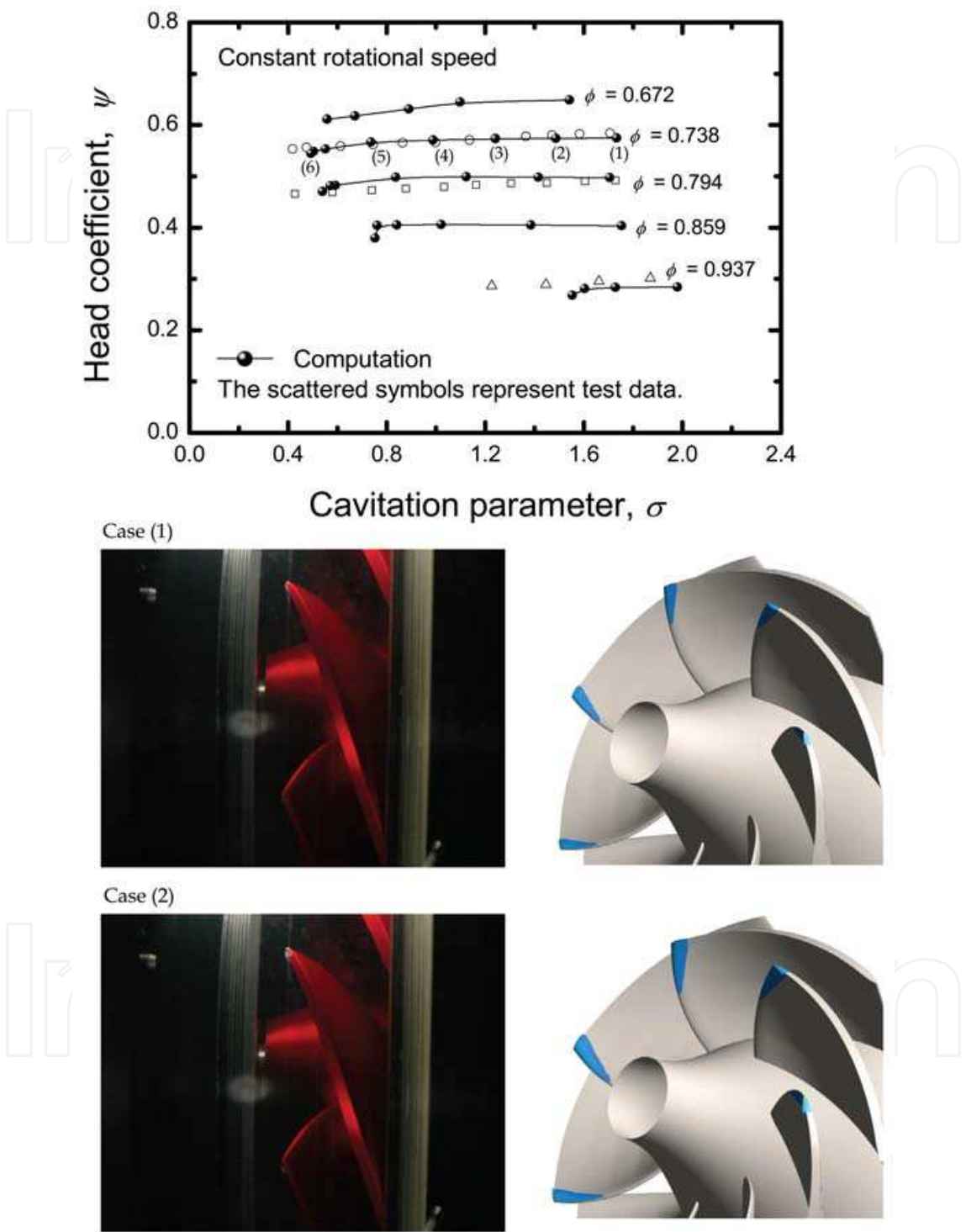


Fig. 10. Cavitation performance characteristics of a mixed-flow pump: NPSH curves

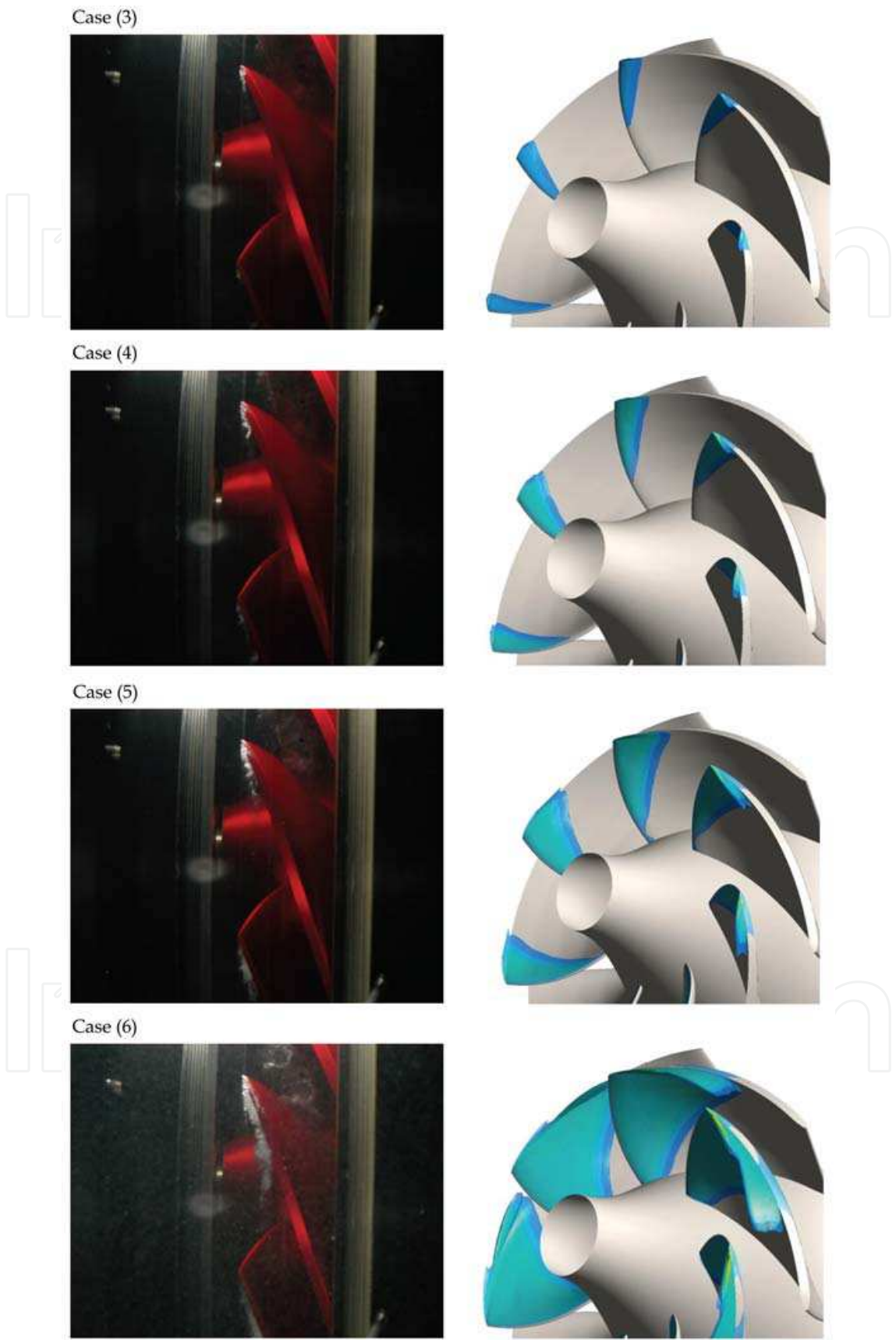


Fig. 10. (continued)



main flow between the impeller blades, extends across the flow channel and consequently leads to a sudden decrease in the total pressure rise. Comparing with the computational results, it is observed that the cavitating region is spread out over the suction surface as well as the leading edge of the impeller blade. By repeating the above procedure for several off-design flowrates under the same rotational speed, the suction performance curves, NPSH versus pump head, have been constructed as shown in Fig. 10. It can be seen that the cavitation performance curves predicted by the CFD code are in good agreement with the measured data. Meanwhile, it is worth noting that the cavitation on the diffuser blade surface has not appeared for the cavitating flow regimes, which means that the diffuser blade design, taking the flow angle leaving the rotating impeller into account, has been successfully carried out in this study.

Every pump has a critical NPSH, i.e. the required net positive suction head ( $NPSH_R$ ), which is defined as the minimum NPSH necessary to avoid cavitation in the pump. Typically, the  $NPSH_R$  is defined as the situation in which the total head decreases by some arbitrarily selected percentage, usually about 3 to 5%, due to cavitation. Although the pump system operates under the NPSH safety margin, it does not ensure the absence of cavitation, i.e. there might be light cavitation that does not give rise to severe hardware damage. However, further reduction in the  $NPSH_R$  will lead to a major deterioration in the hydraulic performance.

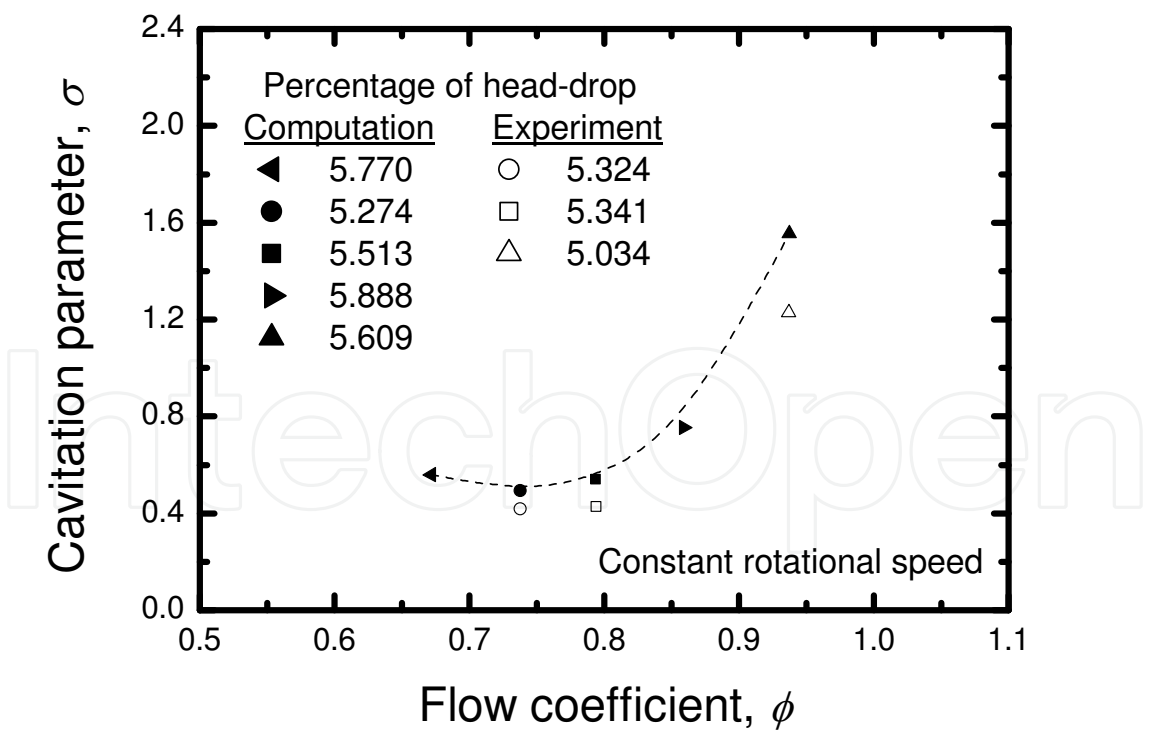


Fig. 11. Cavitation performance characteristics of a mixed-flow pump:  $NPSH_R$  curve



This article employs an about 5% head-drop criterion to define the  $NPSH_R$  for a mixed-flow pump. Figure 11 shows the performance characteristic curves for the  $NPSH_R$  under the operating flowrate conditions. From this figure, it is noted that the  $NPSH_R$  for a newly designed pump with the highest pump efficiency is minimized near the design flowrate regime.

## 5. Conclusions

A practical design and performance analysis procedure of a mixed-flow pump, in which the conceptual approach to turbomachinery design using the meanline analysis is followed by the detailed design and analysis based on the verified CFD code, has been presented in this Chapter. Performance curves predicted by a coupled CFD code were compared with the experimental data of a designed, hydrodynamically efficient, mixed-flow pump. The results agree fairly well with the measured performance curves over the entire operating conditions. A study for the cavitation performance characteristic curves of a mixed-flow pump has also been successfully carried out, although further research is definitely needed to suppress the tip-vortex cavitation under the normal condition.

The design and predictive procedure, including cavitation, employed throughout this study can serve as a reliable tool for the detailed design optimization and assist in the understanding of the operational characteristics of general purpose hydraulic and compressible flow turbomachinery.

## 6. Acknowledgements

The author would like to thank Dr. E S YOON of the Korea Institute of Machinery and Materials (KIMM) for his advice and support and it is also gratefully acknowledged that Dr. K S KIM and Dr. J W AHN of the Maritime and Ocean Engineering Research Institute (MOERI) provide the experimental data for a mixed-flow pump to publish this Chapter.

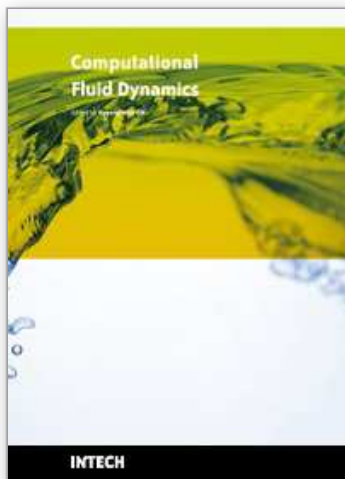
## 7. References

- Aungier, R. H. (2000). *Centrifugal Compressors: A Strategy for Aerodynamic Design and Analysis*, American Society of Mechanical Engineers Press, ISBN 0791800938, New York
- Balje, O. E. (1981). *Turbomachines: A Guide to Design, Selection, and Theory*, John Wiley, ISBN 0471060364, New York
- Japikse, D. (1994). *Introduction to Turbomachinery*, Concepts ETI, ISBN 0933283067, Norwich
- Neumann, B. (2005). *The Interaction between Geometry and Performance of a Centrifugal Pump*, John Wiley, ISBN 0852987552, New York
- Oh, H. W. & Kim, K-Y. (2001). Conceptual design optimization of mixed-flow pump impellers using mean streamline analysis. *Proc. IMechE, Part A: J. Power and Energy*, 215, A1, 133-138, ISSN 09576509

Stepanoff, A. J. (1993). *Centrifugal and Axial Flow Pumps: Theory, Design, and Application*, Krieger Publishing Company, ISBN 0894647237, Florida

IntechOpen

IntechOpen



## **Computational Fluid Dynamics**

Edited by Hyoung Woo Oh

ISBN 978-953-7619-59-6

Hard cover, 420 pages

**Publisher** InTech

**Published online** 01, January, 2010

**Published in print edition** January, 2010

This book is intended to serve as a reference text for advanced scientists and research engineers to solve a variety of fluid flow problems using computational fluid dynamics (CFD). Each chapter arises from a collection of research papers and discussions contributed by the practiced experts in the field of fluid mechanics. This material has encompassed a wide range of CFD applications concerning computational scheme, turbulence modeling and its simulation, multiphase flow modeling, unsteady-flow computation, and industrial applications of CFD.

### **How to reference**

In order to correctly reference this scholarly work, feel free to copy and paste the following:

Hyoung Woo OH (2010). Application of Computational Fluid Dynamics to Practical Design and Performance Analysis of Turbomachinery, Computational Fluid Dynamics, Hyoung Woo Oh (Ed.), ISBN: 978-953-7619-59-6, InTech, Available from: <http://www.intechopen.com/books/computational-fluid-dynamics/application-of-computational-fluid-dynamics-to-practical-design-and-performance-analysis-of-turbomac>

**INTECH**  
open science | open minds

### **InTech Europe**

University Campus STeP Ri  
Slavka Krautzeka 83/A  
51000 Rijeka, Croatia  
Phone: +385 (51) 770 447  
Fax: +385 (51) 686 166  
[www.intechopen.com](http://www.intechopen.com)

### **InTech China**

Unit 405, Office Block, Hotel Equatorial Shanghai  
No.65, Yan An Road (West), Shanghai, 200040, China  
中国上海市延安西路65号上海国际贵都大饭店办公楼405单元  
Phone: +86-21-62489820  
Fax: +86-21-62489821

© 2010 The Author(s). Licensee IntechOpen. This chapter is distributed under the terms of the [Creative Commons Attribution-NonCommercial-ShareAlike-3.0 License](https://creativecommons.org/licenses/by-nc-sa/3.0/), which permits use, distribution and reproduction for non-commercial purposes, provided the original is properly cited and derivative works building on this content are distributed under the same license.

IntechOpen

IntechOpen